UNLIMITED

(2)

AD-A213 419

RSRE
MEMORANDUM No. 4289

ROYAL SIGNALS & RADAR ESTABLISHMENT

A WELL CONDITIONED FORMULATION FOR THE ANALYSIS OF MULTI-LAYERED FREQUENCY SELECTIVE SURFACES USING A CASCADED MATRIX APPROACH

Authors: A J Mackay & J G Gallagher

PROCUREMENT EXECUTIVE,
MINISTRY OF DEFENCE,
R S R E MALVERN,
WORCS.

89 10 16 149

UNLIMITED

RSRE MEMORANDUM No. 4289

CONDITIONS OF RELEASE

0051801 BR-111531

.... U

.... Y

Reports quoted are not necessarily available to members of the public or to commercial organisations.

RSRE MEMORANDUM 4289

Title: A WELL CONDITIONED FORMULATION FOR THE ANALYSIS OF MULTI-LAYERED FREQUENCY SELECTIVE SURFACES USING A CASCADED MATRIX APPROACH

Author: Andrew Mackay and J G Gallagher

Date: May 1989

ABSTRACT

A general method to analyse multi-layered Frequency Selective Surfaces is given which includes a full coupling of evanescent and decaying modes in a well conditoned manner. The method is capable of analysing arbitrary lossy dielectric and magnetic materials used as supports with partially conducting (Salisbury) surfaces and is valid for incident plane waves with arbitrary polarisation and angles of incidence.

The solution is obtained by modal matching of the fields in the apertures of each surface in a manner which satisfies the boundary conditions using Galerkin testing. One important feature is the manner in which the cascaded matrices are put together to avoid numerical problems.

Theoretical predictions have been made on a wide range of surfaces and tested against experiment with satisfactory results.

A WELL CONDITIONED FORMULATION FOR THE ANALYSIS OF MULTI-LAYERED FREQUENCY SELECTIVE SURFACES USING A CASCADED MATRIX APPROACH

Andrew Mackay and J G Gallagher

INTRODUCTION

Frequency selective surfaces have many possible uses as filters, polarisers and for radomes and in other electromagnetic structures. In many instances, single layer surfaces might be suitable and for many others a multi-layer surface can be designed from a knowledge of the Transmission and Reflection coefficient of the single surfaces in isolation. This latter approach is often referred to as a simple scattering matrix (SMA) analysis and is valid provided there is no evanescent mode coupling between layers [1]. However, there will be many instances where evanescent mode coupling must be taken into account when the layers are a sufficiently small fraction of a wavelength apart. Indeed, there is no reason to suppose that multi-layer frequency selective surfaces can not be explicitly designed to utilise this strong coupling. In such a design procedure it is clearly desirable to have a method for calculating the properties of such strongly bound layered structures with a fair degree of confidence.

Shuley [2] considered a generalisation of the SMA to allow for complete interaction by the use of evanescent mode coupling. Similar methods have been used later by Cwik and Mittra [3], Hall, Mittra and Mitzner [4] and Christodoulou et al [5].

In order to use an exact Floquet modal analysis it is necessary to construct a unit cell common to all layers of the surface so that the entire structure is periodic with respect to this global unit cell. This is only unnecessary if there is insignificant evanescent mode coupling between surfaces and in this case surfaces do not need to share a common periodicity. In general, any periodic surface can be constructed from a (global) unit cell represented as a parallelogram illustrated in fig 1.1 below

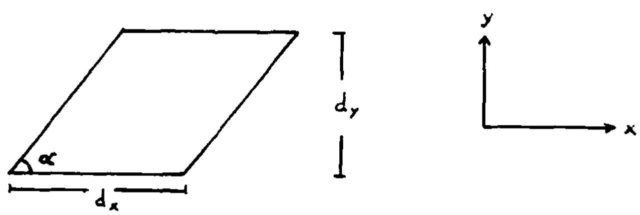

Figure 1.1

All fields generated by the FSS must thus be periodic with respect to the Floquet modal values

$$u_{pq} = k_o \sin\theta_o \cos\varphi_o + \frac{2\pi p}{d_x} \tag{1a}$$

$$v_{pq} = k_o \sin\theta_o \sin\varphi_o + \frac{2\pi q}{d_y} - \frac{2\pi p}{d_x \tan\alpha} \tag{1b}$$

where p,q are integers of either sign, $k_o = 2\pi/\lambda_o$ is the wavenumber of the incident field in free space, and θ_o and φ_o are the angles of incidence of the plane wave as illustrated in Fig 1.2 below:

FSS in x-y plane

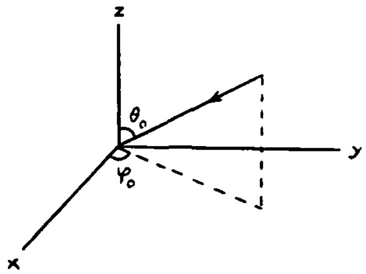

Figure 1.2

It should be noted that these Floquet modes are common to <u>all</u> the layers of the FSS, independent of any dielectric or magnetic material values since the value of φ_o is unchanged within the structure and $k.\sin\theta$ is unchanged by Snell's law throughout the structure (where k is the wavenumber in any layer of the multilayer structure, and θ is the direction of incidence - complex for a lossy material - within that layer).

The modal fields have an x,y dependence proportional to $\exp(-j[u_{pq}x + v_{pq}y])$ and a z-dependence proportional to $\exp(-j\gamma_{pq}z)$ where

$$\gamma_{pq} = \sqrt{\epsilon_r \mu_r k_o^2 - u_{pq}^2 - v_{pq}^2} \qquad (2)$$

and when an implicit time dependence $e^{j\omega t}$ is assumed. ϵ_r, μ_r are possibly complex with a negative imaginary part representing loss and γ_{pq} is taken so that the imaginary part $\mathrm{Im}(\gamma_{pq}) \leqslant 0$ to ensure correct behaviour as $z \to +\infty$ (assuming all distances are taken in a positive sense).

The electric field may be decomposed into orthonormal Transverse Electric and Transverse Magnetic vector Floquet Modal Fields $\underline{\varphi}_{pqr}$ with r = 1 representing TE and r = 2 representing TM modes, so that

$$\underline{\varphi}_{pqr} = \begin{cases} \dfrac{1}{\sqrt{d_x d_y}} \left[\dfrac{v_{pq}}{t_{pq}} \hat{\underline{x}} - \dfrac{u_{pq}}{t_{pq}} \hat{\underline{y}} \right] \varphi_{pq}, & r = 1 \text{ (TE)} \\[2ex] \dfrac{1}{\sqrt{d_x d_y}} \left[\dfrac{u_{pq}}{t_{pq}} \hat{\underline{x}} + \dfrac{v_{pq}}{t_{pq}} \hat{\underline{y}} \right] \varphi_{pq}, & r = 2 \text{ (TM)} \end{cases} \qquad (3)$$

where $$t_{pq} = \sqrt{v_{pq}^2 + u_{pq}^2} \tag{4}$$

$$\psi_{pq} = \exp\left[-j\left[u_{pq}x + v_{pq}y\right]\right] \tag{5}$$

We apply the electric and magnetic field boundary conditions by considering convenient canonical structures with which we build the complete multi-layer structure. For example, an FSS interface backed by a single layer of material (as used by Chen [6]) may be used. Alternatively, only a single interface may be used. The latter approach is adopted for programming convenience which will be efficient whenever any dielectric layer is sandwiched by FSS conducting structures on both sides. Choosing this approach, any arbitrary multi-layered FSS may therefore be constructed from the two canonical structures illustrated below.

Case (1)

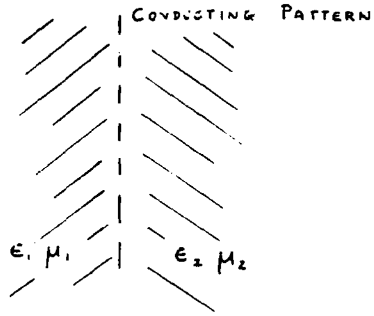

Figure 2.1

where a metal FSS pattern is bounded on either side by materials with different bulk electrical characteristics for ϵ_r and μ_r. (Resistive patterns may also be considered - see Hall, Mittra and Mitzner [4])

Case (2)

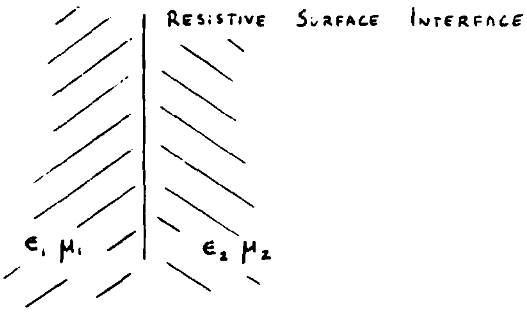

Figure 2.2

where there is a resistive (possibly not present) layer of zero thickness bounded on either side by two different electrical materials

These two structures, when separated by any thickness of uniform material in any combination can be used to represent any multi-layer FSS of conducting elements, resistive screens and arbitrary supporting materials, as illustrated in the example figure below, Fig 2.3.

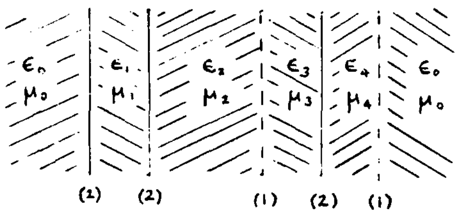

Figure 2.3

where each interface may be represented as an example of a canonical structure (1) or a structure (2). In this paper, we choose to propagate the electric field through from one layer to the next.

We now show how to relate the (electric) fields on either side of the interface of a canonical structure.

BOUNDARY CONDITIONS AT AN FSS INTERFACE

We first consider the interface of canonical structure (1). Using a generalised scattering matrix approach, the field to either side of the interface can be written as the sum of incoming and outgoing modal fields.

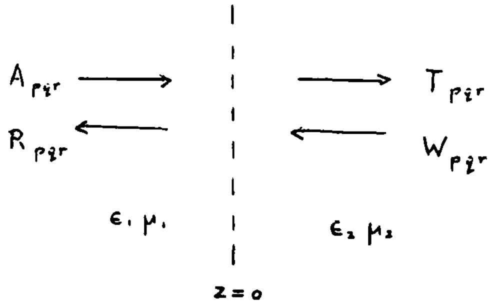

Just to the left of the interface, the total tangential electric field, $\underline{E}^{-}_{t}$ may be written as

$$E_t^- = \begin{cases} \sum\limits_{pqr} A_{pqr}\,\varphi_{pqr}(\underline{x}) + \sum\limits_{pqr} R_{pqr}\,\varphi_{pqr}(\underline{x}), & \underline{x} \in \text{FSS aperture} \\ 0, & \underline{x} \notin \text{FSS aperture} \end{cases} \qquad (6)$$

where $\underline{x}$ is evaluated at the interface $z = 0$ and the metal pattern can be resolved into regions of conductor (no aperture) and regions of no conductor (aperture). Similarly, on the right of the interface, the total tangential electric field, $\underline{E}^{+}_{t}$ may be written as

$$\underline{E}_t^{+} = \begin{cases} \sum\limits_{pqr} T_{pqr}\, \varphi_{pqr}(\underline{a}) + \sum\limits_{pqr} W_{pqr}\, \varphi_{pqr}(\underline{x}) \ , & \underline{x} \in \text{FSS aperture} \\ 0, & \underline{x} \notin \text{FSS aperture} \end{cases} \tag{7}$$

where

$$\sum_{pqr} \equiv \sum_{p=-P_{max}}^{P_{max}} \sum_{q=-Q_{max}}^{Q_{max}} \sum_{r=1}^{2} \ ,$$

P_{max} and Q_{max} are sufficiently large and where A_{pqr}, R_{pqr}, T_{pqr}, W_{par} are complex constants representing incident reflected transmitted and returning wave mode coefficients respectively. We may now apply the tangential boundary condition across a magnetic/dielectric interface; $\underline{E}_t$ is continuous over the aperture. Since the tangential field is zero elsewhere on both sides, we can write

$$\sum_{pqr} A_{pqr}\, \varphi_{pqr}(\underline{x}) + \sum_{pqr} R_{pqr}\, \varphi_{pqr}(\underline{x}) = \sum_{pqr} T_{pqr}\, \varphi_{pqr}(\underline{x}) + \sum_{pqr} W_{pqr}\, \varphi_{pqr}(\underline{x})$$

$$\text{for } \underline{x} \text{ everywhere on interface} \tag{8}$$

We may now also apply the condition that the tangential <u>magnetic</u> field is also continuous over the aperture (but <u>not</u> over the conductor). On the left hand side, the total tangential magnetic field is given (following a generalisation of Chen [6]) by

$$-\hat{\underline{z}} \times \underline{H}^{-} = \sum_{pqr} A_{pqr}\, \xi^{(1)}_{pqr}\, \varphi_{pqr}(\underline{x}) - \sum_{pqr} R_{pqr}\, \xi^{(1)}_{pqr}\, \varphi_{pqr}(\underline{x}) \tag{9}$$

and on the right hand side by

$$-\hat{\underline{z}} \times \underline{H}^{+}_{t} = \sum_{pqr} T_{pqr}\, \xi^{(2)}_{pqr}\, \varphi_{pqr}(\underline{x}) - \sum_{pqr} W_{pqr}\, \xi^{(2)}_{pqr}\, \varphi_{pqr}(\underline{x}) \tag{10}$$

where $\xi^{(i)}{}_{pqr}$ are the modal admittances in region (i) given by

$$\xi^{(1)}_{pqr} = \begin{cases} \dfrac{\gamma^{(1)}_{pq} \sqrt{\dfrac{\epsilon_o}{\mu_o}}}{\mu^{(1)}_r k_o} \quad , \quad r = 1 \text{ (TE)} \\[2em] \dfrac{\epsilon^{(1)}_r k_o \sqrt{\dfrac{\epsilon_o}{\mu_o}}}{\gamma^{(1)}_{pq}} \quad , \quad r = 2 \text{ (TM)} \end{cases} \tag{11a}$$

where

$$\gamma^{(1)}_{pq} = \sqrt{\epsilon^{(1)}_r \mu_r^{(1)} k_o^2 - t^2_{pq}} \tag{11b}$$

and

$$\xi^{(2)}_{pqr} = \begin{cases} \dfrac{\gamma^{(2)}_{pq}}{\mu^{(2)}_r k_o} \sqrt{\dfrac{\epsilon_o}{\mu_o}} \quad , \quad r = 1 \text{ (TE)} \\[2em] \dfrac{\epsilon^{(2)}_r k_o}{\gamma^{(2)}_{pq}} \sqrt{\dfrac{\epsilon_o}{\mu_o}} \quad , \quad r = 2 \text{ (TM)} \end{cases} \tag{12a}$$

where

$$\gamma^{(2)}_{pq} = \sqrt{\epsilon^{(2)}_r \mu^{(2)}_r k_o^2 - t^2_{pq}} \tag{12b}$$

combining (9) and (10) we now have

$$\sum_{pqr} A_{pqr}\, \xi^{(1)}_{pqr}\, \varphi_{pqr}(\underline{x}) - \sum_{pqr} R_{pqr}\, \xi^{(1)}_{pqr}\, \varphi_{pqr}(\underline{x})$$

$$= \sum_{pqr} T_{pqr} \xi^{(2)}_{pqr} \varphi_{pqr}(\underline{x}) - \sum_{pqr} W_{pqr} \xi^{(2)}_{pqr} \varphi_{pqr}(\underline{x}) \quad , \ \underline{x} \in \text{aperture only} \tag{13}$$

Equations (8) and (13) may now be solved in the following manner. Firstly, the orthogonal properties of φ_{pqr} may be used in conjunction with (8) to write

$$A_{pqr} + R_{pqr} = T_{pqr} + W_{pqr} \quad \forall \quad p,q,r \tag{14}$$

(This may be shown by forming the dot product of (8) with $\underline{e}^*_{k\ell m}$ and integrating over the whole unit cell). Substituting (14) into (13) yields

$$2 \sum_{pqr} A_{pqr} \xi^{(1)}_{pqr} \underline{e}_{pqr}(\underline{x}) = \sum_{pqr} T_{pqr} \left[\xi^{(1)}_{pqr} + \xi^{(2)}_{pqr}\right] \underline{e}_{pqr}(\underline{x})$$

$$+ \sum_{pqr} W_{pqr} \left[\xi^{(1)}_{pqr} - \xi^{(2)}_{pqr}\right] \underline{e}_{pqr}(\underline{x})$$

$$\underline{x} \in \text{aperture only} \tag{15}$$

If we write the total tangential electric field at the interface by $\underline{E}_t$, then an alternative use of the orthogonality condition with (8) is that

$$T_{pqr} + W_{pqr} = \iint_{\text{aperture}} \underline{E}_t(\underline{x}) \cdot \underline{e}^*_{pqr}(\underline{x}) \, da \tag{16}$$

Substituting (16) into (15) provides a more useful formulation in terms of the total tangential electric field given by

$$2 \sum_{pqr} A_{pqr} \xi^{(1)}_{pqr} \underline{e}_{pqr}(\underline{x}) = \sum_{pqr} \left[\xi^{(1)}_{pqr} + \xi^{(2)}_{pqr}\right] \underline{e}_{pqr}(\underline{x}) \iint_{\text{aperture}}$$

$$\underline{E}_t(\underline{x}') \cdot \underline{e}^*_{pqr}(\underline{x}') da'$$

$$- 2 \sum_{pqr} W_{pqr} \xi^{(2)}_{pqr} \underline{e}_{pqr}(\underline{x})$$

$$\underline{x} \in \text{aperture only} \tag{17}$$

$\underline{E}_t$ ($\underline{x}$) can be written as a completely arbitrary expansion of basis functions [6] which are only required to be linearly independent over the aperture under the inner product

$$\langle \underline{A}, \underline{B} \rangle = \iint_{\text{aperture}} \underline{A}(\underline{x}) \cdot \underline{B}^*(\underline{x}) \, da \tag{18}$$

so that we may write

$$\underline{E}_t(\underline{x}) = \sum_{mn\ell} F_{mn\ell}\underline{\psi}_{mn\ell}(\underline{x}) \quad , \quad \underline{x} \in \text{aperture} \tag{19}$$

Note that the inner product (18) implicitly assumes that $\underline{E}_t(\underline{x})$ is zero when $\underline{x} \notin$ aperture, and thus (19) requires $\underline{\psi}_{mn\ell}(\underline{x})$ only to be defined over the aperture. In practice, $\underline{\psi}_{mn\ell}$ may be chosen as the electric field slot modes for a slotted structure (or as the fields caused by the expected current modes in an element structure) thus ensuring as few $\underline{\psi}_{mn\ell}$ as possible for good convergence to the solution. In order to solve (17) given a set of $\underline{\psi}_{mn\ell}$ we may assume Galerkin testing, substitute (19) into (17), form the dot product of (17) with $\underline{\psi}^*_{MNL}(\underline{x})$ and integrate over the unit cell (with $\underline{\psi}^*_{MNL}(\underline{x})$ defined as zero for $\underline{x} \notin$ aperture). This yields the set of equations

$$2\left\{I_{MNL}\right\} = \left\{Y^{mn\ell}_{MNL}\right\}\left\{F_{mn\ell}\right\} - 2\left\{\Omega_{MNL}\right\} \tag{20}$$

where

$$I_{MNL} = \sum_{pqr} A_{pqr}\,\xi^{(1)}_{pqr}\,C^{*MNL}_{pqr} \tag{21}$$

$$Y^{mn\ell}_{MNL} = \sum_{pqr}\left[\xi^{(1)}_{pqr} + \xi^{(2)}_{pqr}\right] C^{*MNL}_{pqr} C^{mn\ell}_{pqr} \tag{22}$$

$$\Omega_{MNL} = \sum_{pqr} W_{pqr}\,\xi^{(2)}_{pqr}\,C^{*MNL}_{pqr} \tag{23}$$

and where

$$C^{MNL}_{pqr} = \iint_{\text{aperture}} \underline{\psi}_{MNL}(\underline{x}') \cdot \underline{\psi}^*_{pqr}(\underline{x}')\,da' \tag{24}$$

In order to employ matrix notation the subscripts (or superscripts) MNL ($mn\ell$) in (20)-(24) will be tabled by a single index $i(j)$ so that $\{I_{MNL}\} = \{I_i\}$, $\{Y_{MNL}{}^{mn\ell}\} = \{Y_{ij}\}$ etc. We may thus write the vector of values $\underline{I} = \{I_i\}$, etc, and the matrix of values $Y = \{Y_{ij}\}$, etc. (20)-(24) now become

$$\underline{I} = C^{\dagger}E^{(1)}\underline{A} \quad , \qquad E^{(1)} = \text{diagonal matrix, diag}\left\{\xi^{(1)}_i\right\}$$

$$\underline{A} = \left\{A_i\right\}$$

$$C = \left\{C_{ij}\right\}$$

$$C^{\dagger} = \left\{C^*_{ji}\right\}$$

$$Y = C^{\dagger}\left[E^{(1)} + E^{(2)}\right]C, \qquad E^{(2)} = \text{diag}\left\{\xi^{(2)}_i\right\}$$

$$\underline{\Omega} = C^{\dagger}E^{(2)}\underline{W}\ , \qquad \underline{W} = \{W_i\}\ , \quad \underline{F} = \{F_i\}$$

so that (20) may be rewritten in matrix notation as

$$2C^{\dagger}E^{(1)}\underline{A} = C^{\dagger}\left[E^{(1)} + E^{(2)}\right] C\,\underline{F} - 2C^{\dagger}E^{(2)}\underline{W} \tag{25}$$

Note that there is a very important feature in this equation; C is in general rectangular so that neither its inverse or the inverse of $C^{\dagger}$ exist. Indeed, even when C is square it is likely to be extremely ill conditioned if sufficiently many Floquet modes are taken into account (ie P_{max} and Q_{max} are sufficiently large). This seems to be a general feature of most frequency selective surfaces; the excited modal fields and currents always span a significantly smaller set than the set of permissible Floquet modes might allow.

Substituting (19) into (16) and using matrix notation with $\{T_{pqr}\} = \{T_i\} = \underline{T}$, yields

$$\underline{T} + \underline{W} = C\,\underline{F} \tag{26}$$

substituting (26) into (25) gives the matrix equation

$$2C^{\dagger}E^{(1)}\underline{A} = C^{\dagger}\left[E^{(1)} + E^{(2)}\right]\underline{T} + C^{\dagger}\left[E^{(1)} - E^{(2)}\right]\underline{W} \tag{27}$$

which together with (14) in vector notation,

$$\underline{A} + \underline{R} = \underline{T} + \underline{W} \tag{28}$$

gives us the general connection matrix between electric fields on the left and right hand side of the interface,

$$\begin{bmatrix} \underline{T} \\ \underline{R} \end{bmatrix} = \begin{bmatrix} 2QE^{(1)} & 2QE^{(2)} - I \\ 2QE^{(1)} - I & 2QE^{(2)} \end{bmatrix} \begin{bmatrix} \underline{A} \\ \underline{W} \end{bmatrix} \tag{29}$$

where I is the identity matrix and

$$Q = C\,Y^{-1}C^{\dagger} \tag{30}$$

Note here that Y^{-1} exists, but Q^{-1} does <u>not</u> exist in general. It is at this stage that an important point should be noted; in general, it is <u>not</u> possible to reorganise (29) to achieve $\underline{T}$ and $\underline{W}$ on one side of the equation and $\underline{A}$ and $\underline{R}$ on the other because of this inversion problem. This seems to be assumed possible in the cascade formulations [4],[5] in order to calculate a composite transmission matrix. If the block matrix in (29) is suitably truncated (ie Q is suitably truncated) it may be possible to invert Q (and thus reorganise (29)) but such a procedure may be very dangerous because the original Q is rank deficient. What is required is a scheme that does not involve the inversion of Q. Cwik and Mittra [3] describe one such method while the authors will describe another.

BOUNDARY CONDITIONS AT A RESISTIVE SHEET

We now consider the second canonical interface (2), and asume a resistive sheet of $1/\sigma_s$ Ohms per square between two electrical media

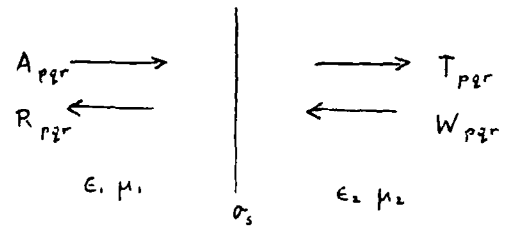

In this case there is no cross coupling between modal fields and thus a surface current

$$J_{pqr} = \sigma_s E^{(t)}_{pqr} \tag{31}$$

is impressed on the surface where

$$E^{(t)}_{pqr} = A_{pqr} + R_{pqr} = T_{pqr}\ W_{pqr} \tag{32}$$

since the tangential electric field is still continuous across the interface.

We now have a discontinuity in the tangential magnetic field given by

$$\left[\epsilon^{(1)}_{pqr} A_{pqr} - \epsilon^{(1)}_{pqr} R_{pqr}\right] - \left[\epsilon^{(2)}_{pqr} T_{pqr} - \epsilon^{(2)}_{pqr} W_{pqr}\right] = J_{pqr} \tag{33}$$

thus, assuming the previous matrix notation where $\{E_i^{(1,2)}\} = \{\epsilon_{pqr}^{(1,2)}\}$, then (31), (32) and (33) may be combined to give us

$$
\begin{bmatrix} \underline{I} \\ \underline{R} \end{bmatrix} = \begin{bmatrix} \mathrm{diag}\left\{2\left[E_i^{(1)} + E_i^{(2)} + E_i^{(2)} + \sigma_s\right]^{-1} E_i^{(1)}\right\} & \mathrm{diag}\left\{\left[E_i^{(1)} + E_i^{(2)} + \sigma_s\right]^{-1}\left[E_i^{(1)} - E_i^{(1)} - \sigma_s\right]\right\} \\ \mathrm{diag}\left\{\left[E_i^{(1)} + E_i^{(2)} + \sigma_s\right]^{-1}\left[E_i^{(1)} - E_i^{(2)} - \sigma_s\right]\right\} & \mathrm{diag}\left\{2\left[E_i^{(1)} + E_i^{(2)} + \sigma_s\right]^{-1} E_i^{(2)}\right\} \end{bmatrix} \begin{bmatrix} \underline{A} \\ \underline{W} \end{bmatrix}
$$

As opposed to (29), (34) is a matrix whose elements may be properly inverted if required. However, since this may not be done with (29) a method must be found to connect matrices of this form which does not require a reorganisaiton. Such a method is illustrated below.

CONNECTION OF MATRICES WITHIN A GENERAL CASCADED SYSTEM

A cascade system that does not require the inversion of the matrix Q in (30) may be constructed. This has the further advantage that evanescent modal fields and fields within a lossy dielectric can be organised in such a way that they always appear to decay in the numerical implementation for arbitrary thicknesses of dielectric. This means that the number of evanescent connections between interfaces can be highly overspecified without causing any ill-conditioning of the scheme. The method proceeds by a grouping of two contiguous canonical interfaces separated by a dielectric/magnetic spacer to form a single composite structure whose form is also that of (29) and (34). This composite structure is then taken together with the next canonical interface and the method repeated in a systematic fashion over the entire multi-layer structure. The grouping of two contiguous structures is illustrated below in Fig 3.

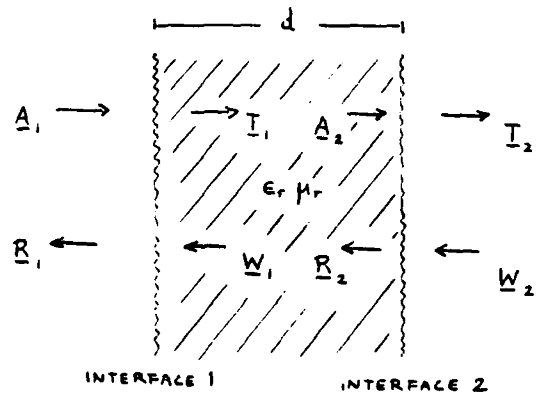

Figure 3

Suppose

$$\begin{bmatrix} \underline{I}_1 \\ \underline{R}_1 \end{bmatrix} = \begin{bmatrix} X'_{11} & X'_{12} \\ X'_{21} & X'_{22} \end{bmatrix} \begin{bmatrix} \underline{A}_1 \\ \underline{W}_1 \end{bmatrix} \tag{35}$$

and

$$\begin{bmatrix} \underline{I}_2 \\ \underline{R}_2 \end{bmatrix} = \begin{bmatrix} X''_{11} & X''_{12} \\ X''_{21} & X''_{22} \end{bmatrix} \begin{bmatrix} \underline{A}_2 \\ \underline{W}_2 \end{bmatrix} \tag{36}$$

where X_{ij}' and X_{ij}'' are known but non-invertible and $\underline{W}_1$ and $\underline{A}_2$ are unknown quantities. In general, if the material between interface (1) and (2) is ϵ_r, μ_r separated by a distance d, then

$$\underline{A}_2 = H\, \underline{I}_1 \tag{37}$$

$$\underline{W}_1 = H\, \underline{R}_2 \tag{38}$$

where

$$H = \mathrm{diag}\left\{\exp\left[+\, j\gamma_i\, d\right]\right\} \tag{39}$$

where

$$\left\{\gamma_i\right\} \equiv \left\{\gamma_{pq\ell}\right\}$$

and

$$\gamma_{pq\ell} = \sqrt{\epsilon_r \mu_r k_o^2 - t_{pq}^2} \tag{40}$$

defined so that $\gamma_{pq\ell}$ (independent of ℓ) is defined with $\mathrm{Im}(\gamma_{pq\ell}) \leq 0$. Equations (35), (36), (37) and (38) may be combined as

$$\underline{I}_1 = \left[X'_{11}\underline{A}_1 + X'_{12}\, H\, X''_{22}\, \underline{W}_2\right] + X'_{12}\, H\, X''_{21}\, H\, \underline{I}_1 \tag{41}$$

We may thus write

$$\underline{I}_1 = (I - L)^{-1}\, \underline{a} \tag{42}$$

where

$$\underline{a} = X'_{11}\underline{A}_1 + X'_{12}\, H\, X''_{22}\, \underline{W}_2 \tag{43}$$

and

$$L = X'_{12}\ H\ X''_{21}\ H \tag{44}$$

Thus, even though L^{-1} may not exist, $(I - L)^{-1}$ does exist and is well conditoned.

We can now obtain $\underline{T}_2$ and $\underline{R}_1$ as

$$\begin{bmatrix} \underline{T}_2 \\ \underline{R}_1 \end{bmatrix} = \begin{bmatrix} Z_{11} & Z_{12} \\ Z_{21} & Z_{22} \end{bmatrix} \begin{bmatrix} \underline{A}_1 \\ \underline{W}_2 \end{bmatrix} \tag{45}$$

where

$$Z_{11} = X''_{11}\ H(I - L)^{-1}\ X'_{11} \tag{46}$$

$$Z_{12} = X''_{11}\ H(I - L)^{-1}\ X'_{12}\ H\ X''_{22} + X''_{12} \tag{47}$$

$$Z_{21} = X'_{21} + X'_{22}\ H\ X''_{21}\ H\ (I - L)^{-1}\ X'_{11} \tag{48}$$

$$Z_{22} = \left\{X'_{22}\ H\ X''_{21}\ H(I - L)^{-1}\ X'_{12} + X'_{22}\right\} H\ X''_{22} \tag{49}$$

With $\underline{T}_2$ and $\underline{R}_1$ obtained from the first two interfaces, the next interface is treated using its own conneciton matrix and that just generated via (45) to construct a new conneciton matrix uisng the same method as outlined above. This proceeds until there are no more interfaces in which case we have a final incoming $\underline{W} = 0$ and $\underline{T}$ and $\underline{R}$ are the final required vectors of the composite structure. The method differs from that of Cwik and Mittra [3] in two important respects. Firstly, the matrix H never appears in an inverted form so exponential terms never cause numerical problems by becoming too large and secondly, our approach uses electric fields rather than power waves.

In this formulation it may immediately be seen that interactions between any pair of interfaces in fig 3 are coupled through the propagation equations (32) and (38). This means that the sizes of the $\underline{T}_1$, $\underline{A}_2$, $\underline{W}_1$ and $\underline{R}_2$ may be limited in size to encompass only those evanescent modes whose decay (described by H) is non-negligible over the distance d. We may further note that $\underline{A}_1$, $\underline{R}_1$ and $\underline{T}_2$, $\underline{W}_2$, may both be of different lengths in the situation where distances between interfaces vary greatly in size (so that the same number of evanescent modes is not required to couple each interface). In fact, this will generally be required since usually only the zero-order modal coefficients will be required in the air region to either side of the composite FSS. This will then result in the matrices X_{ij}', X_{ij}'' and Z_{11} and Z_{22} being rectangular.

One possible scheme that may be imposed is to set an automatic threshold $0 < T < 1$ and to limit the matrix size so that only those modes p,q,r are taken in determining the size of $\underline{T}_1$, $\underline{A}_2$, $\underline{W}_1$ and $\underline{R}_2$ such that $\exp[+j\gamma_{pqr}d] < T$ from (39),(40).

TRANSMISSION AND REFLECTION S-MATRICES AND ENERGY BALANCE

Once the final $\underline{T}$ and $\underline{R}$ are known in terms of the initial vector $\underline{A}$, the problem is almost solved. Usually, the final quantities required are the transmitted and reflected electric fields in the $\hat{\varphi}$ and $\hat{\theta}$ directions given an incident wave of unit amplitude and arbitrary polarisation incident at the angle (φ_0, θ_0). With such a full polarimetric description it is convenient to describe a polarisation coordinate system in the direction of the wave.

Let us write the incident electric field by

$$\underline{E}_o = \alpha_\varphi \hat{\underline{\varphi}}_o + \alpha_\theta \hat{\underline{\theta}}_o = \begin{bmatrix} \alpha_\varphi \\ \alpha_\theta \end{bmatrix} \tag{50}$$

with

$$\begin{aligned} \hat{\underline{\varphi}}_o &= -\sin\varphi_o\,\hat{\underline{x}} + \cos\varphi_o\,\hat{\underline{y}} \\ \hat{\underline{\theta}}_o &= \cos\varphi_o\cos\theta_o\,\hat{\underline{x}} + \sin\varphi_o\cos\theta_o\,\hat{\underline{y}} - \sin\theta_o\,\hat{\underline{z}} \end{aligned} \tag{51}$$

the reflected wave has an angle of reflection $\theta_{refl} = \theta_o$, $\varphi_{refl} = \pi + \varphi_o$, but the wave is directed away rather than towards the surface. Thus define

$$\begin{aligned} \hat{\underline{\varphi}}_{refl} &= \hat{\underline{\varphi}}_o \\ \hat{\underline{\theta}}_{refl} &= -\hat{\underline{\theta}}_o \end{aligned} \tag{52}$$

so that

$$\underline{E}_{refl} = \beta_\varphi \hat{\underline{\varphi}}_{refl} + \beta_\theta \hat{\underline{\theta}}_{refl} = \begin{bmatrix} \beta_\varphi \\ \beta_\theta \end{bmatrix} \tag{53}$$

With the transmitted field, the transmission angles $\theta_{tran} = \pi - \theta_o$ $\varphi_{tran} = \pi + \varphi_o$ and the wave is directed in the same direction as the incident wave, thus define

$$\begin{aligned} \hat{\underline{\varphi}}_{tran} &= \hat{\underline{\varphi}}_o \\ \hat{\underline{\theta}}_{tran} &= \hat{\underline{\theta}}_o \end{aligned} \tag{54}$$

so that

$$\underline{E}_{tran} = \gamma_\varphi \hat{\underline{\varphi}}_{tran} + \gamma_\theta \hat{\underline{\theta}}_{tran} = \begin{bmatrix} \gamma_\varphi \\ \gamma_\theta \end{bmatrix} \tag{55}$$

With these definitons, we wish to construct the scattering matrix for transmission given by

$$\underline{E}_{tran} = \begin{bmatrix} t_{11} & t_{12} \\ t_{21} & t_{22} \end{bmatrix} \underline{E}_o \tag{56}$$

and the scattering matrix for reflection given by

$$\underline{E}_{refl} = \begin{bmatrix} r_{11} & r_{12} \\ r_{21} & r_{22} \end{bmatrix} \underline{E}_o \tag{57}$$

It may now be shown that if the final matrix equation (45), produced after all the interfaces have been included, is given by

$$\begin{bmatrix} \underline{I} \\ \underline{R} \end{bmatrix} = \begin{bmatrix} \hat{Z}_{11} & \hat{Z}_{12} \\ \hat{Z}_{21} & \hat{Z}_{22} \end{bmatrix} \begin{bmatrix} \underline{A} \\ 0 \end{bmatrix}$$

with the p = q = 0 terms of $\hat{Z}_{11}$ given by

$$\begin{bmatrix} \hat{z}^{(1)}_{11} & \hat{z}^{(1)}_{12} \\ \hat{z}^{(1)}_{21} & \hat{z}^{(1)}_{22} \end{bmatrix}$$

(for r = 1 and 2 interactions) and with the p = q = 0 terms of Z_{21} given by

$$\begin{bmatrix} \hat{z}^{(2)}_{11} & \hat{z}^{(2)}_{12} \\ \hat{z}^{(2)}_{21} & \hat{z}^{(2)}_{22} \end{bmatrix}$$

(for r = 1 and 2 interactions)

$$\begin{bmatrix} t_{11} & t_{12} \\ t_{21} & t_{22} \end{bmatrix} = \begin{bmatrix} \hat{z}^{(1)}_{11} & -\hat{z}^{(1)}_{12} \cos\theta \\ -\hat{z}^{(1)}_{21}/\cos\theta & \hat{z}^{(1)}_{22} \end{bmatrix} \tag{58}$$

and

$$\begin{bmatrix} r_{11} & r_{12} \\ r_{21} & r_{22} \end{bmatrix} = \begin{bmatrix} \hat{z}^{(2)}_{11} & -\hat{z}^{(2)}_{12} \cos\theta \\ \hat{z}^{(2)}_{21}/\cos\theta & -\hat{z}^{(2)}_{22} \end{bmatrix} \tag{59}$$

furnishing the desired result. If the composite FSS is lossless, we may note that conservation of energy implies

$$|t_{11}|^2 + |t_{21}|^2 + |r_{11}|^2 + |r_{21}|^2 = 1 \tag{60}$$

and

$$|t_{12}|^2 + |t_{22}|^2 + |r_{21}|^2 + |r_{22}|^2 = 1 \tag{61}$$

for arbitrary angles of incidence provided that no higher order grating lobes are excited. This provides a useful check on the calculation. Unfortunately, although a necessary condition (60) and (61) are not a sufficient condition and it is not appropriate to use (60) and (61) to attempt to provide an estimate on, for example, the number of modes required in the program. When losses or grating lobes are present we have the strict inequalities.

$$|t_{11}|^2 + |t_{21}|^2 + |r_{11}|^2 + |r_{21}|^2 < 1$$

$$|t_{12}|^2 + |t_{22}|^2 + |r_{21}|^2 + |r_{22}|^2 < 1$$

and with lossy dielectrics it is often possible to get significant energy absorption.

MEASUREMENTS FACILITY

In order to confirm the method, predictions using this program and experimental measurements of the transmission coefficient using a Vector Network Analyser have been made for a selection of frequency selective surfaces at various angles of incidence and polarisation. The experimental arrangement is illustrated below in Fig 4.

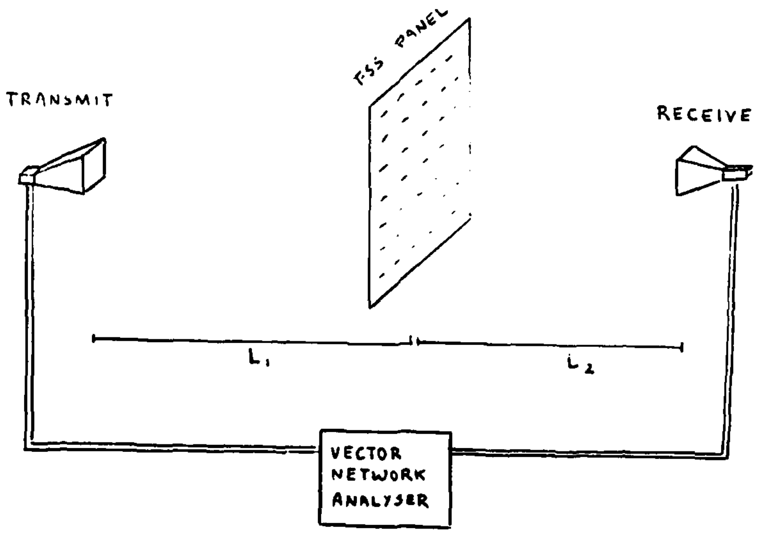

Figure 4

Measurements have been successfully made from 4.5 GHz to 20 GHz in ranges determined by the horns used to transmit and receive. The FSS is about 4 x 4 feet in size, rotatable about its vertical axis and the horns may be rotated so that the $\underline{E}$-field is either vertical or horizontal. The separation distances L_1 and L_2 are of the order of 8 feet providing an approximate far-field plane wave illumination of the screen. Measurements are made with and without the FSS panel and the appropriate vector division is carried out automatically by the VNA providing both power transmission and phase (if required) coefficients of the FSS.

PREDICTIONS AND EXPERIMENTAL COMPARISONS

In the following examples rectangular slotted structures are considered. The reasons for this are that (1) their modes and thus the best choice of field expansion modes $\underline{\psi}'_{pqr}(\underline{x})$ are well known (see, for example Chen [6]) and (2) they are of considerable practical interest for the design of frequency filters that are also required to be polarisation isolating.

Example 1

Consider a single array of slots backed onto a dielectric substrate. The array of slots has a unit cell size (see fig 1.1) with d_x = 17.5mm, d_y = 7.5mm, $\alpha = 41^\circ$ with a single slot per unit cell of length 15.0mm by 1.0mm aligned with respect to the unit cell so that its long dimension is pointing in the $\underline{x}$-dirn. The dielectric backing is standard fibre-glass FR4 material of thickness 1.57mm with an estimated $\mathrm{Re}(\epsilon_r) = 4.0$ and loss tangent $\tan\delta = 0.027$ (These values are assumed in all the numerical predictions by the authors using FR4, and seem the best values to take over the frequency range 7.0 GHz $\rightarrow$ 17.0 GHz).

In the following predictions, the number of Floquet modes used are given by $P_{max} = Q_{max} = 13$, and the expansion modes $\underline{\psi}'_{pqr}$ are chosen as $\underline{\psi}'_{pqr} = \underline{\varphi}_{pqr}$ for q = 0 and $-10 \leqslant p \leqslant 10$. (This is not a good choice for $\underline{\psi}'_{pqr}$ with slots, but is sufficient to illustrate the method). Finally, the number of evanescent modes required to couple the air-dielectric and slotted array interface is taken with an automatic threshold of T = 0.05 at all frequencies and angles of incidence. Figures 5.1 a-c illustrate the predictions and measurements of the power transmission coefficient in db, given by $20\log_{10}|t_{11}|$, over the range 7 to 17 GHz for transverse electric polarisation ($\underline{E}$ directed in the $\underline{y}$-direction) for θ = 0, 10 and 45°, (φ = 0). The continuous curves illustrate the measurements and the dots the predictions. Figures 5.1 d-e illustrate the predictions and measurements for θ = 10°, 45° (φ = 90°) for the transverse magnetic polarisation ($\underline{H}$ directed in the $\underline{x}$-direction) given by $20\log_{10}|t_{22}|$.

Example 2

Consider the same array of slots as used above, but with one on either side of the dielectric substrate. The two arrays are arranged so that there is a lateral offset between them in the $\underline{x}$-direction, but no offset in the y-direction. If 100% offset indicates a lateral shift in a given direction by a complete unit cell, then in this example there is a 50% lateral offset of the slots in the $\underline{x}$-direction (along the axis of the slot).

Figures 5.2 a-c illustrate the predictions and measurements for transverse electric polarisation at θ = 0, 10 and 45°, and figures 5.2 d-e illustrate the predictions and measurements for transverse magnetic polarisation at θ = 10 and 45° as in example 1.

Example 3

Consider 3 arrays of slots, of the kind described above, separated by two thicknesses of FR4 material both of width 1.57mm. In this example, all 3 slot arrays are aligned with each other with no lateral offset. The frequency range examined is from 4.5 GHz to 12 GHz and a figure for the threshold T is chosen as before with T = 0.05 (where it may be noted that about 41 transverse electric and 41 transverse magnetic connecting modes are necessary at 12 GHz). Figures 5.3 a,b,c show predictions and measurements at $\theta = 0^\circ$, $\theta = 10^\circ$ TE and $\theta = 10^\circ$ TM in the sense defined in example 1.

CONCLUSIONS

The method described is the most robust multi-layer FSS method that the authors are aware of with significant accuracy advantages over some other cascade methods. Provided a sufficient number of Floquet modes is chosen together with a sufficiently good set of field expansion functions (necessary criteria for any single layer FSS program) then the method described is well conditioned and capable of high accuracy when (1) there are significantly fewer field expansion functions than evanescent modes and (2) the coupling threshold T is chosen arbitrarily small. The examples presented are by no means special and probably do not have any special practical application, but a more detailed parameter study is currently underway to examine slotted arrays of more interest. This will be reported on in a later article.

ACKNOWLEDGEMENTS

The authors are indebted to David Brammer for his useful suggestions and discussions concerning the improved conditioning of cascaded FSS structures.

REFERENCES

[1] S. W. Lee, G. Zarillo, C. L. Law "Simple formulas for transmission through periodic metal grids or plates" IEEE Trans. 1982. AP-30, pp904-909.

[2] N. V. Shuley "Higher-Order mode interaction in planar periodic structures" IEE Proceedings, Vol. 131, Pt. H, No. 3, June '84, pp 129-132.

[3] T. Cwik, R. Mittra "The Cascade Connection of Planar Periodic Surfaces and Lossy Dielectric Layers to form an arbitrary periodic screen" IEEE Trans A P, Vol. AP-35, No. 12, Dec. '87 pp 1397-1405.

[4] R. C. Hall, R. Mittra, K. Mitzner "Analysis of Multilayered Periodic Structures Using Generalised Scattering Matrix Theory" IEEE Trans AP, Vol. AP-36, No. 4, April '88. pp 511-517.

[5] C. G. Christodoulou, D. P. Kwan, R. Middleveen, P. F. Wahid "Scattering from Stacked Coatings and Dielectrics for various angles of wave incidence" IEEE Trans Anten & Prop., Vol. 36, No. 10, Oct '88.

[6] C. C. Chen "Transmission through a conducting screen perforated periodically with Apertures" IEEE Trans MTT-18, September '79, pp 627-632.

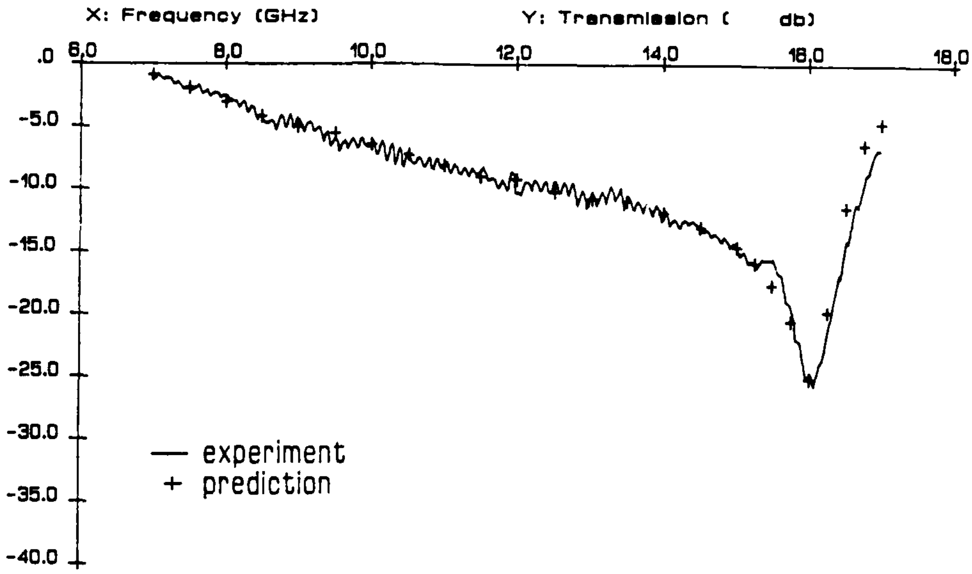

Figure 5.1a FSS Example_1 theta=0 degrees ,(TEM)

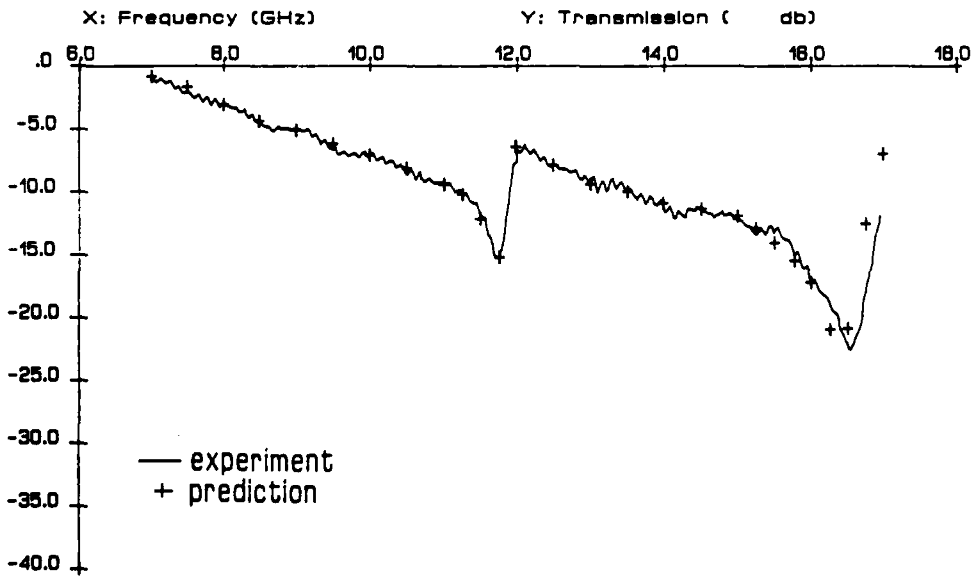

Figure 5.1b FSS Example_1 theta=10 degrees ,(TE)

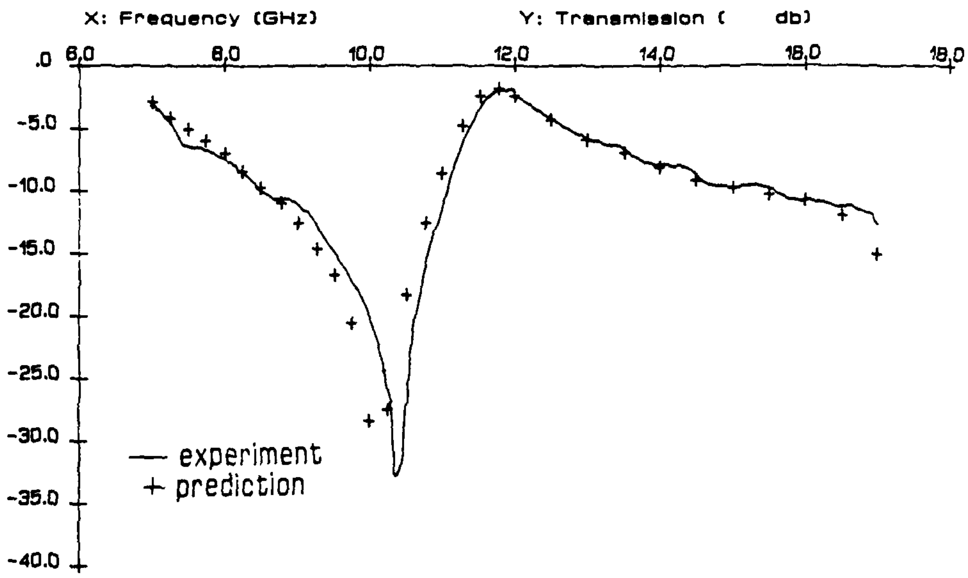

Figure 5.1c FSS Example_1 theta=45 degrees ,(TE)

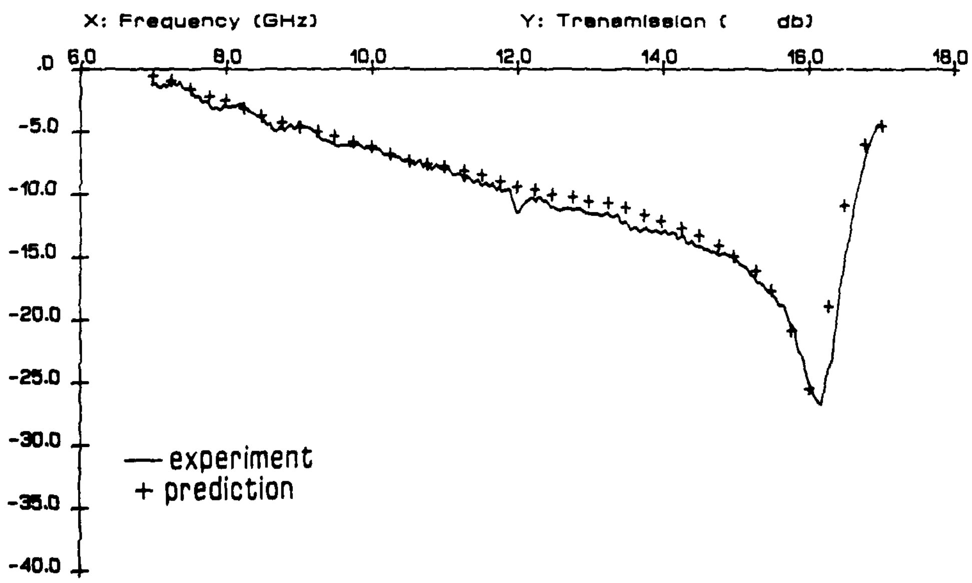

Figure 5.1d FSS Example_1 theta=10 degrees ,(TM)

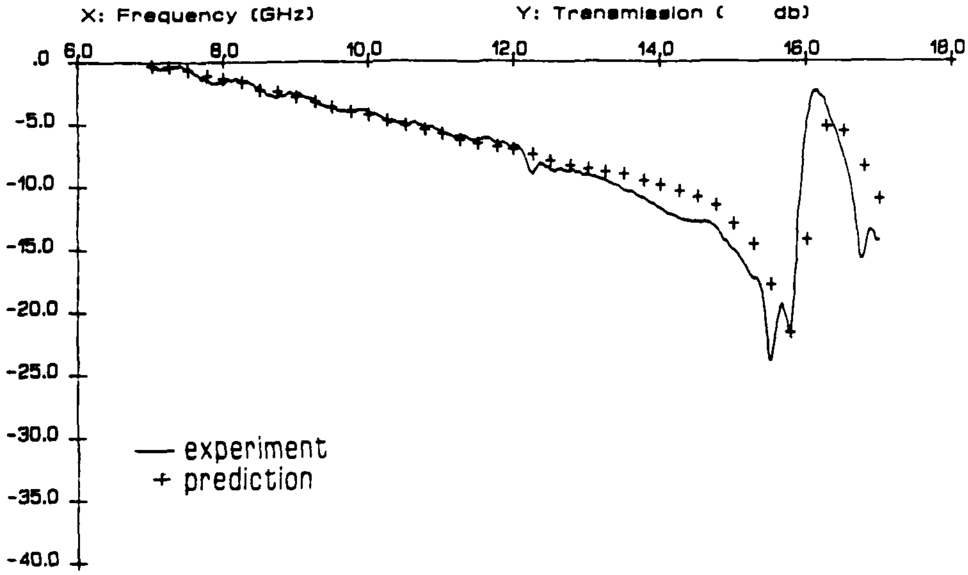

Figure 5.1e FSS Example_1 theta=45 degrees ,(TM)

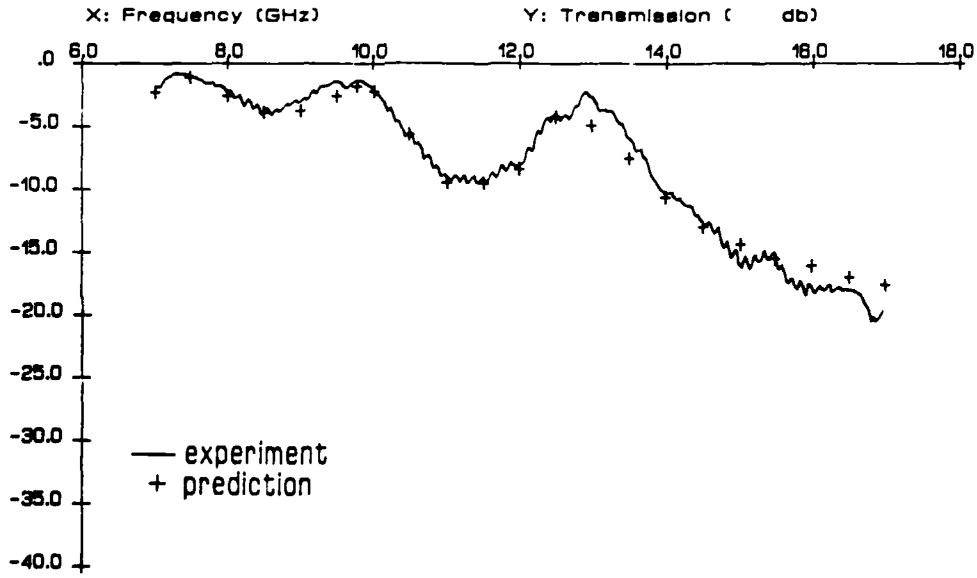

Figure 5.2a FSS Example_2 theta=0 degrees ,(TEM)

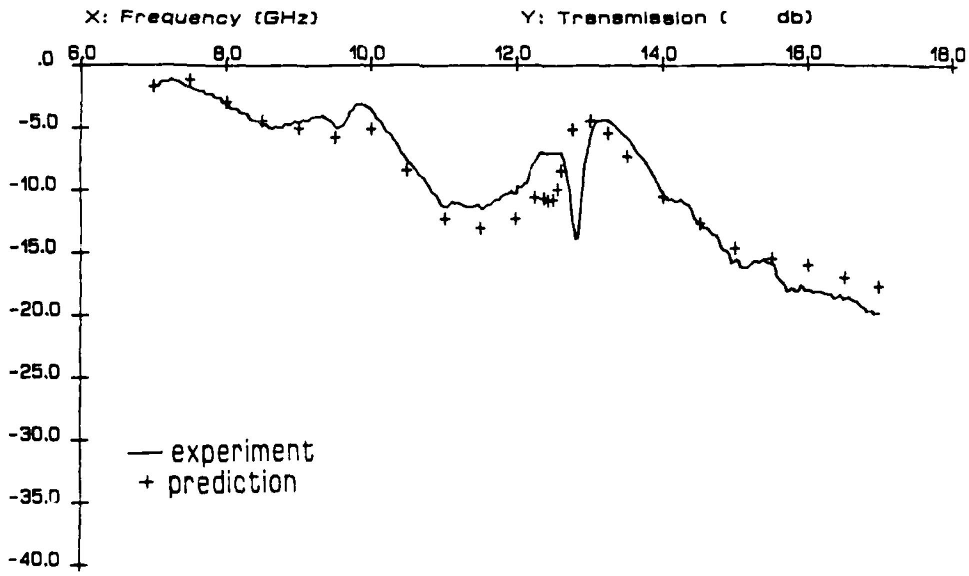

Figure 5.2b FSS Example_2 theta=10 degrees ,(TE)

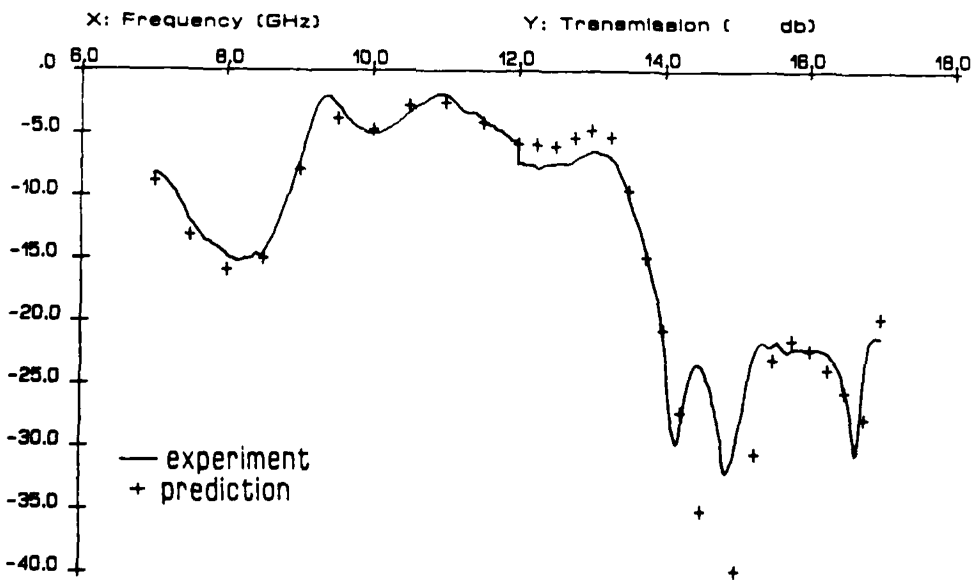

Figure 5.2c FSS Example_2 theta=45 degrees ,(TE)

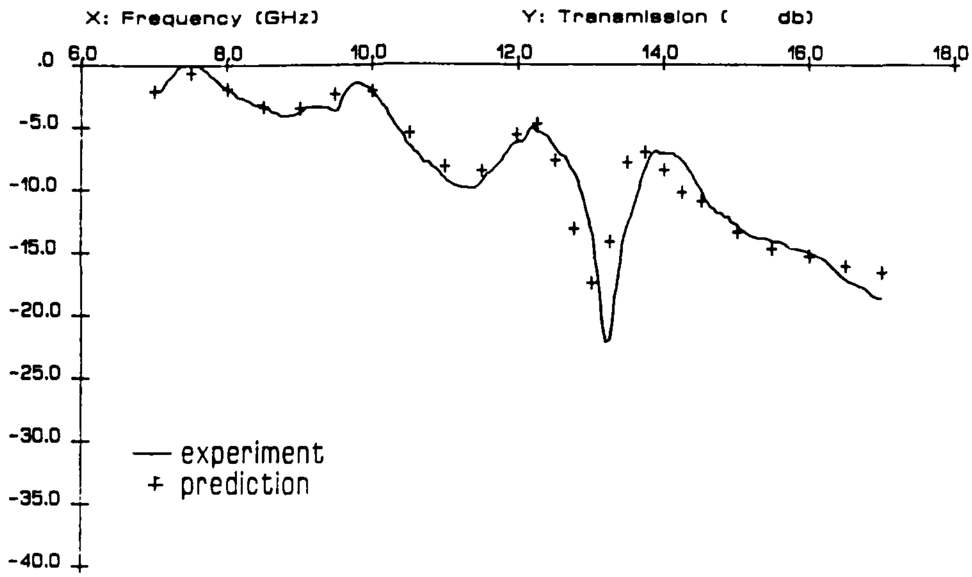

Figure 5.2d FSS Example_2 theta=10 degrees ,(TM)

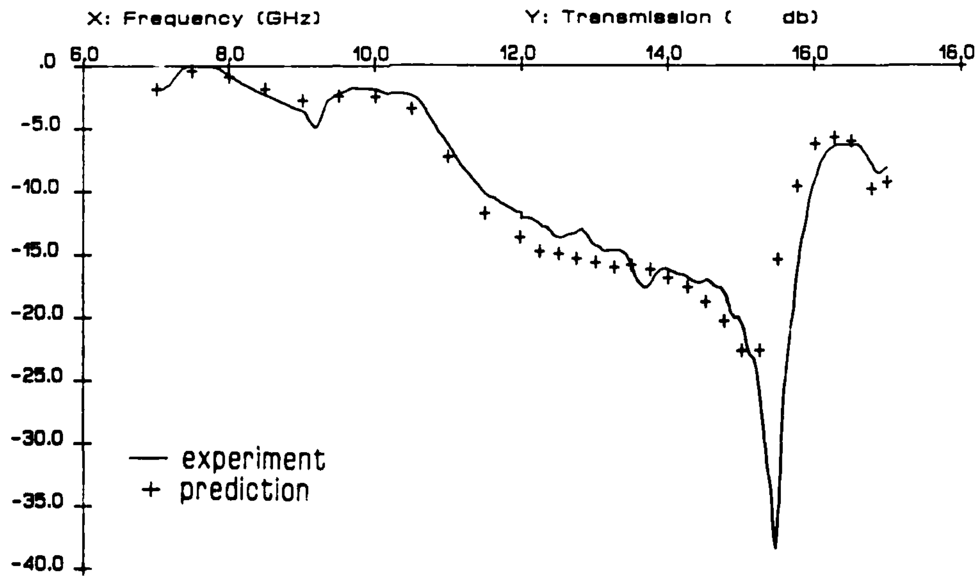

Figure 5.2e FSS Example_2 theta=45 degrees ,(TM)

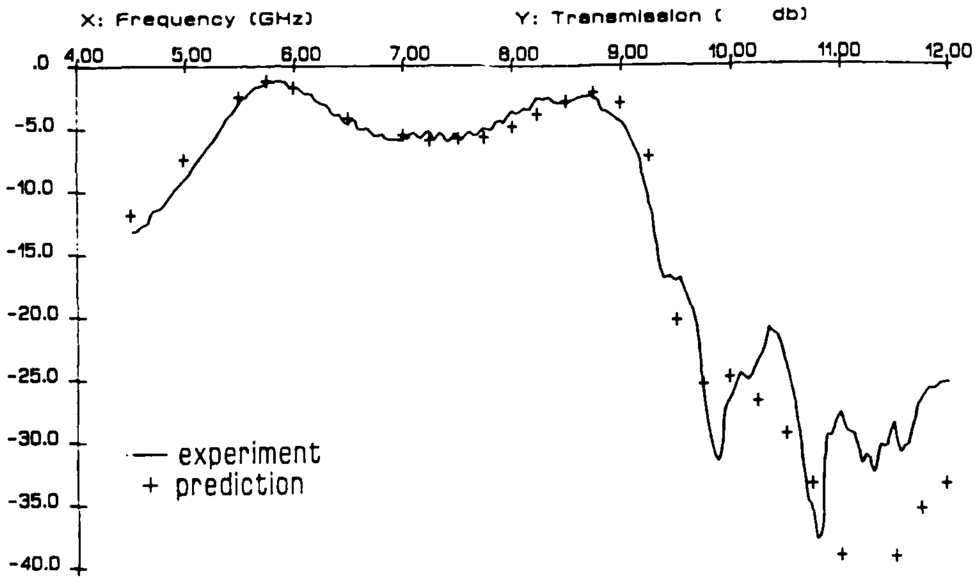

Figure 5.3a FSS Example_3 theta=0 degrees ,(TEM)

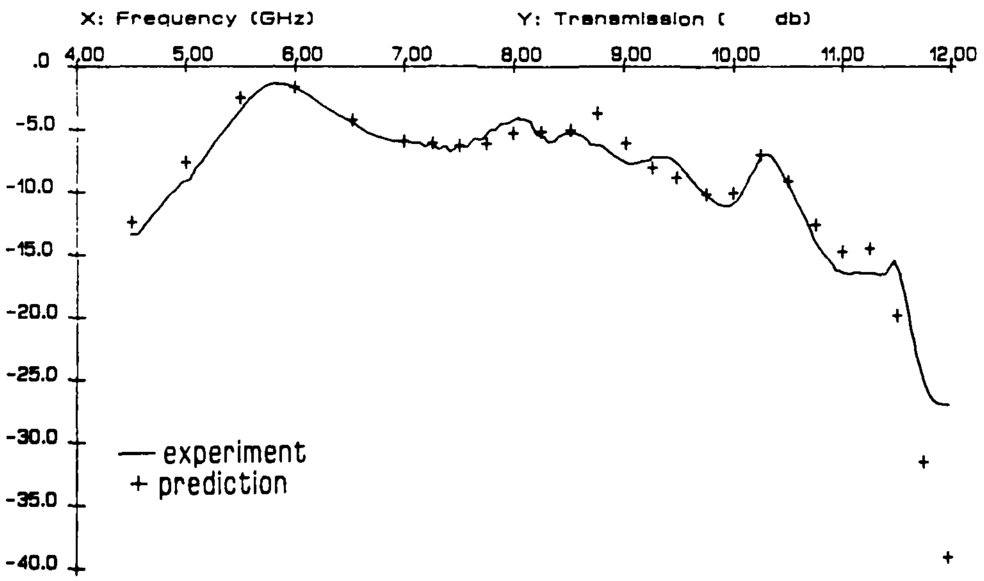

Figure 5.3b FSS Example_3 theta=10 degrees ,(TE)

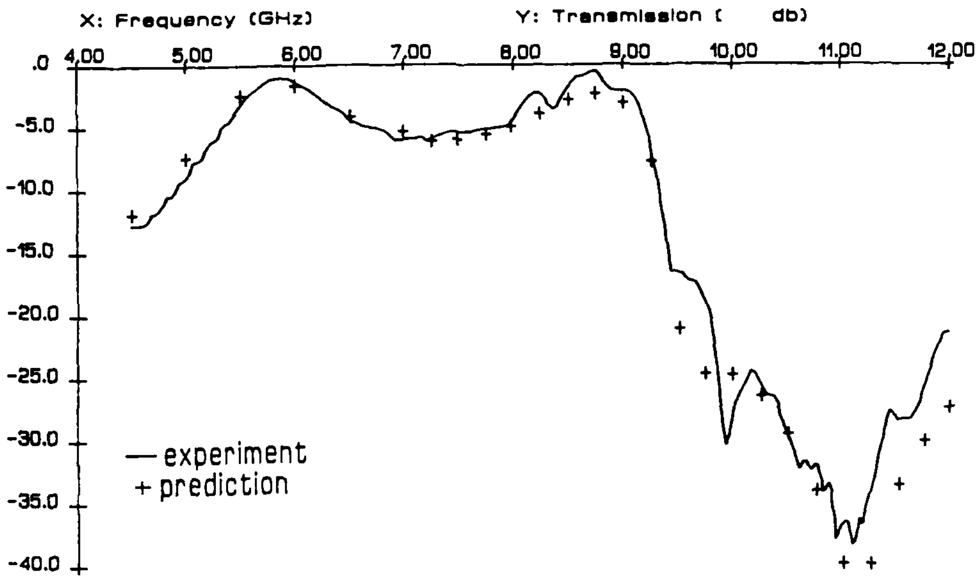

Figure 5.3c FSS Example_3 theta=10 degrees ,(TM)

DOCUMENT CONTROL SHEET

Overall security classification of sheet ......UNCLASSIFIED...

(As far as possible this sheet should contain only unclassified information. If it is necessary to enter classified information, the box concerned must be marked to indicate the classification eg (R) (C) or (S))

1. DRIC Reference (if known)	2. Originator's Reference MEMO 4289	3. Agency Reference	4. Report Security Classification U/C
5. Originator's Code (if known) 7784000	6. Originator (Corporate Author) Name and Location ROYAL SIGNALS AND RADAR ESTABLISHMENT ST ANDREWS ROAD, GREAT MALVERN WORCESTERSHIRE WR14 3PS		
5a. Sponsoring Agency's Code (if known)	6a. Sponsoring Agency (Contract Authority) Name and Location		
7. Title A WELL CONDITIONED FORMULATION FOR THE ANALYSIS OF MULTI-LAYERED FREQUENCY SELECTIVE SURFACES.			
7a. Title in Foreign Language (in the case of translations)			
7b. Presented at (for conference papers) Title, place and date of conference			
8. Author 1 Surname, initials MacKAY A J	9(a) Author 2 GALLAGHER J G	9(b) Authors 3,4...	10. Date 1989.05 pp. ref. 25
11. Contract Number	12. Period	13. Project	14. Other Reference
15. Distribution statement UNLIMITED			
Descriptors (or keywords) continue on separate piece of paper			

Abstract A general method to analyse multi-layered Frequency Selective Surfaces is given which includes a full coupling of evanescent and decaying modes in a well conditioned manner. The method is capable of analysing arbitrary lossy dielectric and magnetic materials used as supports with partially conducting (Salisbury) surfaces and is valid for incident plane waves with arbitrary polarisation and angles of incidence.

The solution is obtained by modal matching of the fields in the apertures of each surface in a manner which satisfies the boundary conditions using Galerkin testing. One important feature is the manner in which the cascaded matrices are put together to avoid numerical problems.

Theoretical predictions have been made on a wide range of surfaces and tested against experiment with satisfactory results.

S80/48